Submitted as a PAPER to IEEE Trans. Ultrason. Ferroelec. & Freq. Contr., August 11, 2006

A Spline Based Approach for Computing Spatial Impulse Responses

Michael A. Ellis
Department of Biomedical Engineering
University of Virginia
mae3x@virginia.edu

Drake Guenther
Department of Biomedical Engineering
University of Virginia
dag2m@virginia.edu

William F. Walker, Ph.D.
Department of Biomedical Engineering
Department of Electrical and Computer Engineering
University of Virginia
bwalker@virginia.edu

Abstract:

Computer simulations are an essential tool for the design of phased array ultrasonic imaging systems. FIELD II, which determines the two-way temporal response of a transducer at a point in space, is the current *de facto* standard for ultrasound simulation tools [1]. However, the need often arises to obtain two-way spatial responses at a single point in time, a set of dimensions for which FIELD II is not well optimized. This paper describes an analytical approach for computing the two-way far-field spatial impulse response from rectangular transducer elements under arbitrary excitation. The described approach determines the response as the sum of polynomial functions, making computational implementation quite straightforward. The proposed algorithm was implemented as a C routine under Matlab and results were compared to those obtained under similar conditions from the well established FIELD II program. Under the specific conditions tested here, the proposed algorithm was approximately 142 times faster than FIELD II for computing spatial sensitivity functions with similar amounts

of error. For temporal sensitivity functions with similar amounts of error, the proposed algorithm was about 1.7 times slower than FIELD II using rectangular elements and 19.2 times faster than FIELD II using triangular elements. DELFI is shown to be an attractive complement to FIELD II, especially when spatial responses are needed at a specific point in time.

Introduction:

The design of modern phased array ultrasonic imaging systems relies heavily on the use of computer simulations. This is necessary because the broadband and near-field nature of most clinical imaging environments severely limits the utility of the Fraunhofer approximation [2] and other theoretical methods. Furthermore, the high degree of optimization of modern systems makes even small deviations from such theory significant. For example, if the system designer is concerned with the array sensitivity pattern down 80 dB from the main-lobe, then a deviation from theory of only 0.1% (-60dB) will significantly affect performance and make optimization to the desired level impossible. Clearly, highly accurate simulation tools are required to guide the selection of transducer geometry, apodization, operating frequency, and other parameters.

While most researchers and designers would agree upon the need for accurate simulation, the appropriate approach depends upon the specific problem of interest and the parameters that are most significant to that problem. For example, in cases where details of transducer vibration and crosstalk are of interest, a computationally costly finite element analysis may be required to capture the most relevant behavior. For such problems the highly optimized PZFlex (Weidlinger Associates, Inc. New York, NY) package is widely used [3]. In other cases, where the detailed transducer response is of less interest, but the propagation medium is inhomogeneous or multiple scattering occurs, the more computationally efficient Finite Difference Method, such as that implemented in Wave2000 (CyberLogic Inc., New York, NY),

may be used [4]. Often, the motivation for adopting more computationally demanding approaches is to account for nonlinear phenomena and inhomogeneities in the simulated environment.

For the vast majority of situations, where the system can be modeled as linear and the propagation medium can be considered homogeneous or inhomogeneities can be modeled as a near-field thin phase screen, Stepanishen's method [5], as implemented in Jørgen Jensen's FIELD II program [1] has become a standard in ultrasound. This approach determines the spatial impulse response of each transmit element, convolves this with the spatial impulse response of each receive element, convolves this result with the transmitted pulse, and finally convolves this with the transmit and receive electromechanical impulse responses to determine the two-way temporal response at a point in space. This technique, as implemented in Jensen's code, has been highly refined over roughly a decade of development so that it is extremely efficient and available in a compiled form on a variety of computer platforms (http://www.es.oersted.dtu.dk/staff/jaj/field/). By computing the temporal signals returned from various target locations, FIELD II readily models common experimental situations.

While the temporal response returned by FIELD II provides an excellent parallel to experiment, recent theoretical work by Zemp [6] and Walker [7] highlights the importance of considering the full four or five dimensional system response. In a previous paper [7], we derive a method for predicting speckle correlation levels for shift variant systems using point spread functions defined as functions of three spatial dimensions and time. While much of this detail is hidden experimentally, the consideration of the full dimensionality of the system response yields insights and offers paths for analysis that are not apparent in the more conventional two dimensional (space, time) view of the system. Zemp [6] carried this concept one step further,

including another dimension for image line index, thereby further clarifying system behavior. Our laboratory has recently applied these frameworks to derive a general resolution metric that allows quantitative comparison of system performance, even when the individual impulse responses of those systems are very different in structure [8]. Interestingly, this new resolution metric is based upon the system response throughout space at a single instant in time; a form of the impulse response that is not naturally determined by FIELD II. Although such responses can be computed by sampling the temporal responses generated by FIELD II, this approach is extremely costly in terms of both computation and storage.

In this paper we describe a new approach to computing spatial impulse responses that directly determines the response throughout space at a single instant in time. This approach is complementary to FIELD II, simply yielding responses in a different set of dimensions. Because results from this code are predictive of system performance and are a permutation of the data available from FIELD II, we name this code DELFI. In this paper we describe the theoretical underpinnings of the DELFI code, describe implementation, and validate the code through comparisons with FIELD II. We discuss the relative computational efficiency of DELFI and discuss future directions for development and refinement.

Theory:

We begin our derivation by considering the general approach employed by Jensen in the FIELD II program [1]. We consider the system response for a specific transmit-receive element pair to be a four dimensional function of space and time:

$$p(x,y,z,t) = e(t) \underset{t}{*} m_t(t) \underset{t}{*} m_r(t) \underset{t}{*} h_t(x,y,z,t) \underset{t}{*} h_r(x,y,z,t) \qquad (1)$$

where x, y, and z are the three spatial dimensions, t is the time for a given line (proportional to range in the beamformed image), $p(x,y,z,t)$ is the system point spread function (psf), $e(t)$ is the electrical excitation of the transmit element, $m_t(t)$ and $m_r(t)$ are the electromechanical transfer functions of the transmit and receive elements respectively, $h_t(x,y,z,t)$ and $h_r(x,y,z,t)$ are the spatial impulse responses of the transmit and receive elements respectively, and $*_t$ indicates convolution in the time dimension. In typical systems the excitation and the transmit and receive electromechanical transfer functions are assumed constant for all elements of the array. Thus we can convolve these terms together before computing the overall response with little loss in generality. Performing this step we simplify (1) to yield:

$$p(x,y,z,t) = emm_{tr}(t) *_t h_t(x,y,z,t) *_t h_r(x,y,z,t) \tag{2}$$

where $emm_{tr}(t)$ is the combined effect of the excitation and the transmit and receive electromechanical transfer functions and can be represented mathematically as $emm_{tr}(t) = e(t) *_t m_t(t) *_t m_r(t)$. While FIELD II computes expressions (1) or (2) using sampled versions of each of the component signals, we take an alternate approach, instead using analytical expressions for these functions.

The utility of an analytical approach depends upon the choice of expressions used: they must be general enough to include all relevant cases, but they must be constrained in such a way to guarantee the presence of an analytical solution. Since (2) allows for consideration of most practically interesting cases and requires two convolutions (rather than the four convolutions of (1)) we build our algorithm upon this expression. Further simplification can be made by

assuming that the point of interest lies in the far-field of both the transmit and receive elements. This is not an onerous assumption since cases where the response would lie in the near-field of a physical element can be readily modeled using a superposition of computational elements for which the far-field assumption is valid. We further simplify the problem by assuming that the elements are rectangular.

Following these assumptions and once again drawing upon the methodology of Jensen [1], we recognize that the one-way spatial impulse response of an element takes on one of three functions. If the field point lies on a line perpendicular to the element face and passing through its center then the spatial impulse response as a function of time is simply a delta function, as shown in the left panel of figure 1. If the field point does not fulfill the first condition, but instead lies upon one of two planes passing through the element center and perpendicular to the element edges then the spatial impulse response in time is a rectangle function, as depicted in the central panel of figure 1. Finally, if the field point fulfills neither of the above conditions then the spatial impulse response in time is a trapezoid function, as shown in the right panel of figure 1. These possible one-way spatial impulse responses are summarized mathematically below. Note we describe the rectangle and trapezoid functions using sums of unit step and ramp functions.

$$h_0(x,y,z,t) = A_0(x,y,z)\delta(t - t_0) \tag{3}$$

$$h_1(x,y,z,t) = A_1(x,y,z)u(t - t_{1,0}) - A_1(x,y,z)u(t - t_{1,1}) \tag{4}$$

$$\begin{aligned} h_2(x,y,z,t) = {} & (t - t_{2,0})A_2(x,y,z)u(t - t_{2,0}) - (t - t_{2,1})A_2(x,y,z)u(t - t_{2,1}) \\ & - (t - t_{2,2})A_2(x,y,z)u(t - t_{2,2}) + (t - t_{2,3})A_2(x,y,z)u(t - t_{2,3}) \end{aligned} \tag{5}$$

where h_0, h_1, and h_2 represent the delta, rectangle, and trapezoid spatial impulse responses respectively and $u(t)$ is the unit step function. The scaling functions $A_0(x,y,z)$, $A_1(x,y,z)$, and $A_2(x,y,z)$ are constant at any specific spatial location and include $1/r$ spreading, scaling to account for the element size, and an obliquity factor to account for a soft transducer baffle [9], if desired. The time delay t_0 present in (3) is determined by the speed of sound and the distance from the element center to the field point. Similarly, the delays present in (4) and (5) are determined from the speed of sound and distances between the field point and the element edges and corners, respectively. It is important to note that these descriptions of the impulse response are only valid in the very far field.

To determine the two-way response from an element pair we must convolve the appropriate version of (3)-(5) for the receive element with the appropriate version of (3)-(5) for the transmit element. While superficial analysis suggests that nine permutations are possible, a more careful examination reveals that since the order of convolution is irrelevant, some of these permutations are redundant. Thus, the two-way response must fit one of the following six general expressions.

$$h_{tr} = h_t \underset{t}{*} h_r = \left\{ h_0 \underset{t}{*} h_0 \text{ or } h_0 \underset{t}{*} h_1 \text{ or } h_0 \underset{t}{*} h_2 \text{ or } h_1 \underset{t}{*} h_1 \text{ or } h_1 \underset{t}{*} h_2 \text{ or } h_2 \underset{t}{*} h_2 \right. \tag{6}$$

where we have dropped space and time references to simplify notation. Note that while the simplified notation of (6) suggests that in some cases (such as $h_2 \underset{t}{*} h_2$) the transmit and receive responses are identical, this is intended only to state that the transmit and receive responses fit the same function; they may have different delays and scaling. Substituting (3)-(5) into (6) yields a set of six possible two-way impulse responses:

$$h_{0_a} \underset{t}{*} h_{0_b} = A_{0_a} A_{0_b} \delta\left(t - t_{0_a} - t_{0_b}\right) \tag{7}$$

$$h_0 \underset{t}{*} h_1 = A_0 A_1 \sum_{j=0}^{1} (-1)^j u\left(t - t_0 - t_{1,j}\right) \tag{8}$$

$$h_0 \underset{t}{*} h_2 = A_0 A_2 \sum_{j=0}^{3} c_j \left(t - t_0 - t_{2,j}\right) u\left(t - t_0 - t_{2,j}\right) \tag{9}$$

$$h_{1_a} \underset{t}{*} h_{1_b} = A_{1_a} A_{1_b} \sum_{j=0}^{1} \sum_{k=0}^{1} (-1)^j (-1)^k \left(t - t_{1_a,j} - t_{1_b,k}\right) u\left(t - t_{1_a,j} - t_{1_b,k}\right) \tag{10}$$

$$h_1 \underset{t}{*} h_2 = A_1 A_2 \sum_{j=0}^{1} \sum_{k=0}^{3} (-1)^j c_k \left(t - t_{1,j} - t_{2,k}\right)^2 u\left(t - t_{1,j} - t_{2,k}\right) \tag{11}$$

$$h_{2_a} \underset{t}{*} h_{2_b} = A_{2_a} A_{2_b} \sum_{j=0}^{3} \sum_{k=0}^{3} c_j c_k \left(t - t_{2_a,j} - t_{2_b,k}\right)^3 u\left(t - t_{2_a,j} - t_{2_b,k}\right) \tag{12}$$

where $c_j = \{1 \text{ for } j = 0 \text{ or } 3 \quad \text{and} \quad -1 \text{ for } j = 1 \text{ or } 2\}$. With each of the six possible two-way impulse responses in hand we can now consider an appropriate analytical representation of the excitation function (including transmit and receive electromagnetic transfer functions). While a number of possible functions are attractive, we choose to represent $emm_{tr}(t)$ using cubic splines [10]. This representation is attractive because it allows arbitrary function shapes while restricting the form of the function to be no higher order than piecewise cubic polynomial. Writing this spline representation explicitly yields:

$$emm_{tr}(t) = \sum_{j=M_0}^{M_1} \left(\alpha_j + \beta_j t + \gamma_j t^2 + \delta_j t^3\right)\left(u\left(t - j\partial\right) - u\left(t - (j+1)\partial\right)\right) \tag{13}$$

where α_j, β_j, γ_j, and δ_j are the spline coefficients, M_0 and M_1 are the first and last spline indices, and $j\partial$ is the spline to spline interval. We can now complete an analytical expression for (2) by convolving (13) with the appropriate version of (7)-(12). While such a convolution appears quite tedious, it can be readily performed utilizing Laplace transforms [11]. The resulting expression is a sum of 3rd, 4th, 5th, 6th, or 7th order polynomials (multiplied by unit step

functions), with the polynomial order depending upon the combination of element responses employed. The analytical forms of these expressions are included in the appendix, although for brevity's sake only one of the summands in each of (8) through (12) is presented. The final expressions can be obtained through superposition of the results from the other summands. Utilizing these final polynomial expressions, the complete two-way response for a given transmit-receive element pair can be computed by simply summing polynomials.

Validation:

The proposed algorithm was implemented in a C routine called as a mex file within Matlab (The Mathworks, Inc. Natick, MA). This approach allowed us to readily generate array geometries and visualize results within Matlab, while taking advantage of the increased computational efficiency of compiled C. All calculations were performed in IEEE Standard double precision floating point arithmetic. All simulations were performed on an IBM x335 with dual Intel Xeon 2.4GHz processors and 2GB PC2100 SDRAM, running Matlab 7.2 under Red Hat Enterprise Linux 3 update 5.

The validity of the proposed algorithm was tested by comparing the two-way spatial response of a single 2D array element as predicted by DELFI, FIELD II using rectangular elements, and FIELD II using triangular elements with a "gold standard". The "gold standard" employed here was the response from FIELD II using triangles, sampled at 10 GHz temporally [12]. Because FIELD II using triangular elements does not make a far-field assumption, it is a very accurate model for the true analytical response and is valid in the near-field. At a sampling rate of 10 GHz, the sharp transitions in the responses are well captured and this method becomes a suitable "gold standard."

For all responses, the array element was modeled using a single 300 x 300 μm computational element. All responses also assumed a combined excitation and transmit/receive electromechanical impulse response equal to a 5.0 MHz sine multiplied by an 8 cycle Nuttall window [13]. This was achieved by windowing a sinusoid and then using the *spline()* command within MATLAB. The system response was determined in polar coordinates over an angle of 0° to 90º (sampled at 0.45°) covering a range from 19.925 cm to 20.075 cm (sampled at 10 μm). This space is an arc of thickness 1.5 mm that exists in the plane perpendicular to the element face, passing through the element center and the center of one of the element edges. Responses were evaluated over this two-dimensional spatial region at a single instant in time (space-space) as well as along the one-dimensional spatial arc in the center of this region throughout time (space-time). Both space-space and space-time responses were evaluated over a range of temporal sampling frequencies from 20 MHz to 1 GHz. For DELFI, all points in the space-space response were computed at the time instant that centered the element response at 20 cm and all points in the space-time response were computed by running the code repeatedly at different time points to generate a waveform at the temporal sampling frequency of interest. For both FIELD II codes, a complete response in range, azimuth, and time was computed, with the time that centered the sensitivity function at 20 cm selected for analysis in the space-space response.

Typical spatial sensitivity functions from DELFI and FIELD II using rectangular elements for the parameters given above are shown in figure 2. Both responses have been normalized to allow comparison. These responses are quite similar except for a series of artifacts located about the 0° line in the FIELD II response. Although the source of this artifact is not apparent, it may result from the corrections FIELD II employs when sampling the infinite

bandwidth spatial impulse responses of the array elements. Such artifacts are avoided in DELFI by evaluating a continuous time representation for the impulse response.

Simulations were performed over a range of temporal sampling frequencies from 20 MHz to 1 GHz to determine computation times and error in the responses as compared to the "gold standard". All computational times were estimated using the tic and toc commands in Matlab. The accuracy of each response was determined by computing the normalized sum squared error with respect to the "gold standard." To ensure proper alignment of the responses when measuring error, time delay estimation was performed using normalized sum squared error with splines [14].

Across the set of 12 space-space simulations, the normalized sum squared errors for DELFI ranged from approximately 1.44% to 0.14%, as shown in figure 3. Over the same set of conditions FIELD II errors ranged from 21.89% to 0.26% using rectangles and 21.05% to 2.02% using triangles. To achieve an error similar to that of DELFI sampled at 40 MHz, FIELD II using rectangles must be sampled at 800 MHz. Comparing computation times at these respective sampling rates, DELFI is about 142 times faster than FIELD II using rectangles. In the sampling range covered, FIELD II using triangles does not achieve an error similar to that of DELFI so such a comparison of computation times was not made. Note that these times do not include any array definitions or other housekeeping operations.

It may seem counterintuitive that FIELD II using triangles – an exact analytical solution that does not make use of a far-field approximation – should have errors as large as 21%. However, we must remember that these impulse responses have sharp transitions that must be appropriately sampled to avoid aliasing errors. The "gold-standard" is sampled temporally at 10

GHz whereas, here, we are considering sampling rates as low as 20 MHz, which result in large aliasing errors in the responses from FIELD II using triangles.

The default sampling rates for DELFI and FIELD II using rectangles are 40 MHz and 100 MHz, respectively. At these rates, these codes have an error of 0.16% and 1.6% and computation times of 0.1 and 5.8 seconds respectively for space-space simulations. So, operating at default sampling frequencies, DELFI is 58 times faster with 10 times less error than FIELD II using rectangles for space-space simulations.

For the sake of comparison we also computed the temporal response using all three codes along the arc 20 cm from the element center, sweeping from 0° to 90° with respect to the line perpendicular to the element face and passing through its center. Across the set of 12 space-time simulations, the normalized sum squared errors for DELFI ranged from approximately 0.76% to 0.04%, as shown in figure 4. Over the same set of conditions FIELD II errors ranged from 19.21% to 0.04% using rectangles and 19.18% to 0.05% using triangles To achieve an error similar to that of DELFI sampled at 40 MHz, FIELD II using rectangles must be sampled at 400 MHz and FIELD II using triangles must be sampled at 300 MHz. Comparing computation times at these respective sampling rates, DELFI is about 1.7 times slower than FIELD II using rectangles and 19.4 times faster than FIELD II using triangles.

Again comparing DELFI and FIELD II using rectangles at their default rates, these codes have an error of 0.06% and 0.78% and computation times of 0.064 and 0.012 seconds, respectively for space-time simulations. So, operating at default sampling frequencies, DELFI is 5.3 times slower with 13 times less error than FIELD II using rectangles for space-time simulations.

Discussion:

Validation of a simulation tool is not a simple task as there is not one method that stands out as the best. As the simulation tool is designed to predict true system behavior, one might argue that comparison to experimental data would serve as the best metric. However, experimental data contains artifacts caused by many non-idealities such as element non-uniformity. Comparing simulation results to experimental data would, thus, produce errors specific to one system. A simulation tool, however, is used to predict general system behavior so such a comparison would not be useful for all readers.

Instead, we have decided to compare our simulation tool one that is well established and makes few assumptions in computing the theoretical field from an ultrasound system. The only assumption made in FIELD II using triangles are that the element is a planar piston vibrating uniformly in an infinite rigid planar baffle into a homogeneous, non-attenuating medium. As a result, the only source of error, aside from those caused by non-idealities, is the temporal sampling frequency, as there are sharp transitions in the impulse response that must be sampled appropriately. As the purpose of a simulation tool is to help steer the decisions of ultrasound system designers by predicting general system behavior, it should be as accurate as possible without becoming too specific to any one system. Thus, FIELD II using triangles was chosen as the "gold standard" from which to determine DELFI's accuracy.

Computing the spatial impulse response of a transmit-receive element pair by convolving (13) with (7)-(12) analytically offers both advantages and disadvantages relative to the established approach using discrete time convolution. On the positive side the analytical approach allows direct computation of the response at a single instant in time. In contrast, the conventional discrete time approach (at least as currently implemented) requires the computation

of a full temporal response even if only a single time point is required. An additional advantage of the analytical approach is that it yields an exact solution, at least within the numerical precision of the computer used for the calculation and within the limitations of the far-field approximation. In contrast, the discrete time approach utilizes under-sampled versions of the element responses and thus introduces some error. In addition, the discrete implementation makes it difficult to compute the spatial response at any exact instant in time. A relative weakness of the analytical approach is that more computation is required to determine a temporal response at a single location.

It should be noted that DELFI is, for the most part, independent of sampling frequency due to its use of an analytical solution. In Figure 3, however, we see that the accuracy of DELFI begins to suffer at a sampling rate of 20MHz. This artifact is due to inaccuracies in the splining of the transmitted pulse for lower sampling frequencies. Although this sampling rate meets the Nyquist criterion, the splined pulse has small errors due to it having too few spline knots. As a result, the accuracy of DELFI suffers for temporal sampling rates that are too close to the Nyquist rate.

The current DELFI code determines the result of the convolution of a single spline segment with two trapezoid functions by summing 16 7^{th} order polynomials. This approach is computationally tedious and subject to numerical instability. Such instabilities occur only when summing the higher order polynomials evaluated at very small time differences. For example, instability occurs when the sides of the trapezoidal responses are very steep or the rectangular response is very narrow in time. To help reduce these instabilities, a minimum time difference parameter is passed into DELFI to determine how the response should be modeled. For example, if the temporal width of rectangle function is smaller than this minimum time

parameter, the response will instead be modeled as a delta function. This would imply that the response would be modeled as a delta function not just along the line through the center of the element, perpendicular to its face, but in a small volume around that line as well. Increasing the minimum time parameter increases this spatial volume. The same spatial broadening occurs for the region in which the response would be modeled as a rectangle function. This approach effectively increases the error in the physical model in order to reduce the much greater numerical error.

An alternative method of implementation that would reduce both numerical instabilities and computation time is to use sums of triangles and rectangles instead of ramps and unit impulses. Using this approach, a trapezoid response would be modeled as two triangles and a rectangle, instead of as four ramp functions. This method will reduce the numerical instabilities in the code by summing polynomials of finite extent rather than those of infinite extent, as currently implemented. This change becomes especially significant with the highest order polynomials, as in (11) and (12), because they tend to saturate the dynamic range of double precision floating point numbers when they are of significant extent. Additionally, this method would provide computational savings by reducing the number of polynomials summed to form a response. The convolution of a single spline segment with two trapezoid functions would involve a summation of 9 seventh order polynomials rather than the 16 required in the current implementation. This approach could cut the computation time nearly in half, although some additional overhead would be required.

Another possible direction for improvement would begin with the recognition that the first half of this response (in time) requires only 8 polynomials for synthesis. Next, by considering the response in negative time it is apparent that the second half of this response

(again in time) also requires only 8 polynomials. Together this realization could cut computation time in half. Additional computational savings are undoubtedly possible.

Algorithmic accuracy could be enhanced by utilizing a more sophisticated model for the element impulse responses. Spline functions might prove particularly suitable for modeling complicated near-field responses [15, 16]. Alternatively, ramp functions or the triangle and rectangle functions described above could be used to form a linear approximation to the more complicated near-field responses. Because DELFI already makes use of ramp functions, such a change would not be major.

A version of DELFI that simulates one-way spatial responses, rather than two-way, has also been written. This version is less susceptible to numerical instabilities due to the use of lower order polynomials. At the time of publication, the source code for both one-way and two-way DELFI will be available on a public web site under a general public license.

Conclusion:

The DELFI code presented here employs analytical convolution of cubic spline functions with continuous time element responses to compute the two-way spatial impulse response of ultrasound transducers. Comparison with FIELD II shows that the proposed algorithm performs comparably to existing methods. For the computation of impulse responses at a single instant in time, the proposed algorithm is about 142 times faster than FIELD II for similar error. For computing temporal responses the proposed code is approximately 1.7 times slower than FIELD II for similar error, although further refinement may reduce this mismatch. When operating at the default sampling frequencies to generate space-space responses, DELFI is 58 times faster with 10 times less error than FIELD II. Generating space-time responses at the default sampling rates, DELFI is 5.3 times slower with 13 times less error than FIELD II. The proposed

algorithm, as implemented by the DELFI code, offers an attractive complement to the well established FIELD II program, especially when spatial responses are needed at a specific point in time.

Acknowledgements:

This work was supported in part by NIH Grant EB002348 and the US Army Congressionally Directed Research Program under Grants DAMD17-01-1-0443 and W81XWH-04-1-0590. The authors would like to thank Karthik Ranganathan for his valuable feedback on this manuscript. The authors would also like to thank IBM for their technical resources and support.

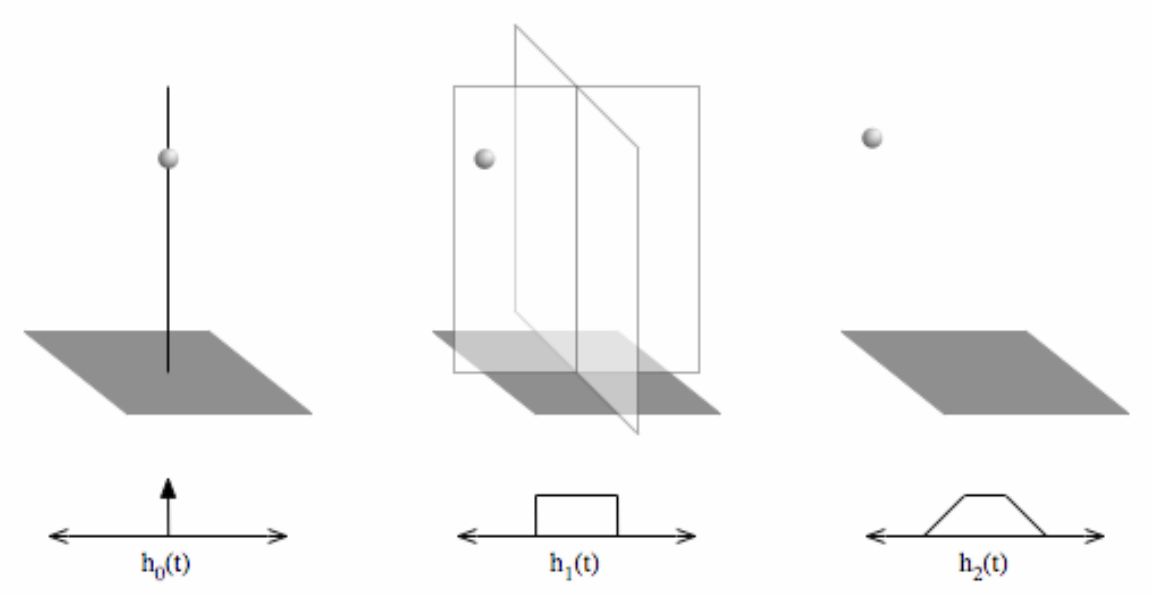

Figure 1:
Geometries for determining the one-way spatial impulse response of an individual array element. In the left panel the field point lies on a line through the element's center and perpendicular to its face. In the center panel the field point does not satisfy the first condition, but lies on a plane that bisects the element and is perpendicular to its face. In the right panel the field point lies at any location not satisfying either of the first two conditions.

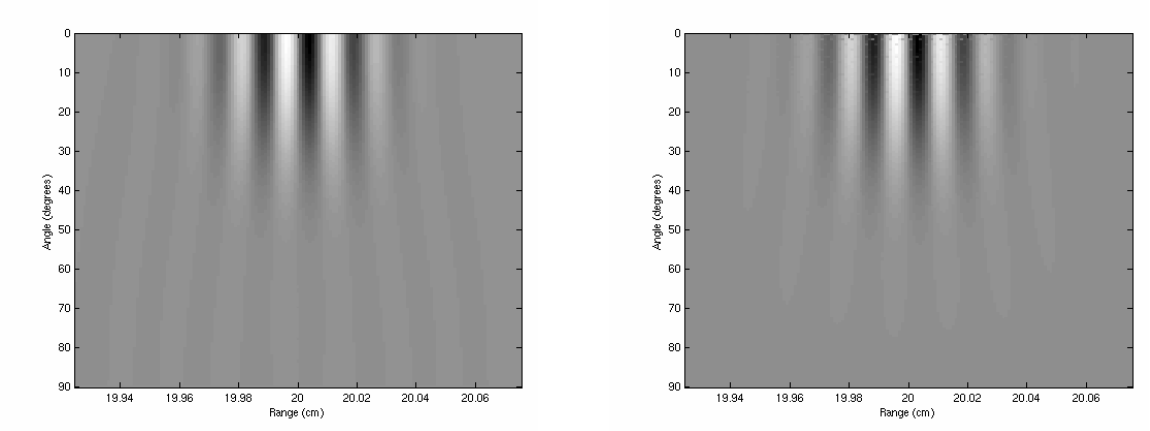

Figure 2:
The spatial impulse response of a 300 μm square array element in a soft baffle for an 8 cycle Nuttall windowed 5.0 MHz transmit pulse. The left panel depicts the output of the proposed algorithm (DELFI) while the right panel indicates the output of FIELD II using rectangles. Both responses have been normalized to allow easy comparison. The responses are nearly identical with the exception of localized artifacts near the 0º line of the FIELD II response.

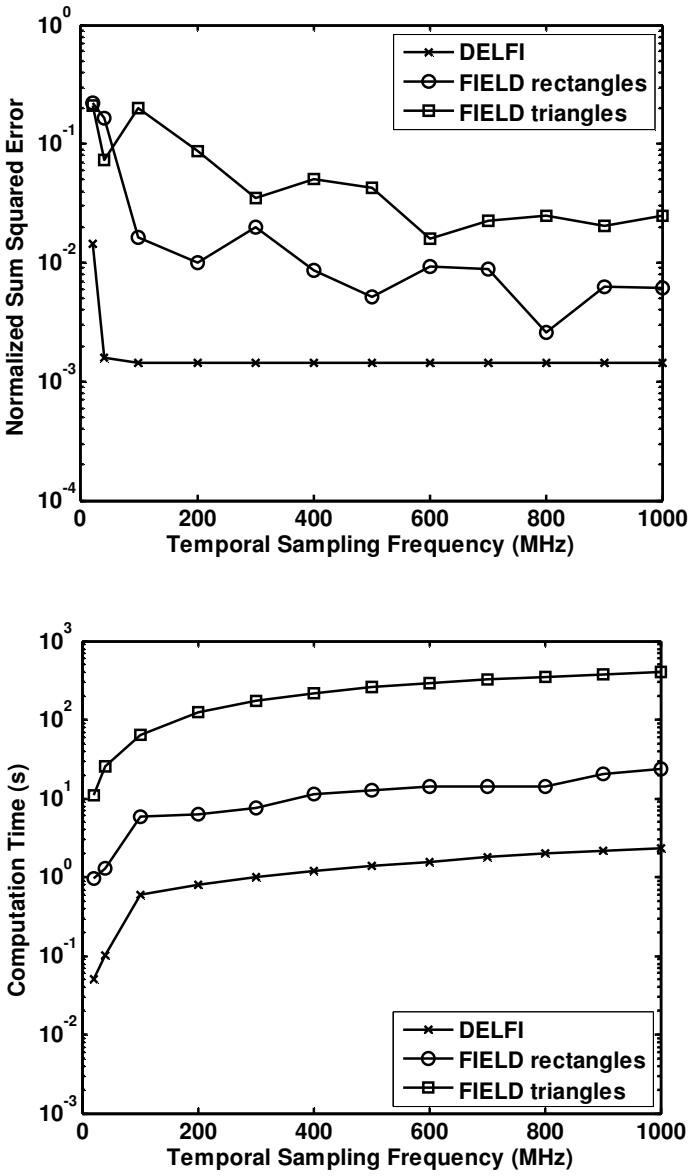

Figure 3:
Comparison of DELFI and FIELD II performance when computing space-space impulse responses over a range of temporal sampling frequencies. The top panel shows the normalized sum squared error with respect to FIELD II using triangles and sampled at 10GHz. The bottom panel shows the computation time for each of the codes. To achieve an error similar to that of DELFI sampled at 40 MHz, FIELD II using rectangles must be sampled at 800 MHz. Comparing computation times at these respective sampling rates, DELFI is about 142 times faster than FIELD II using rectangles. In the sampling range covered, FIELD II using triangles does not achieve an error similar to that of DELFI.

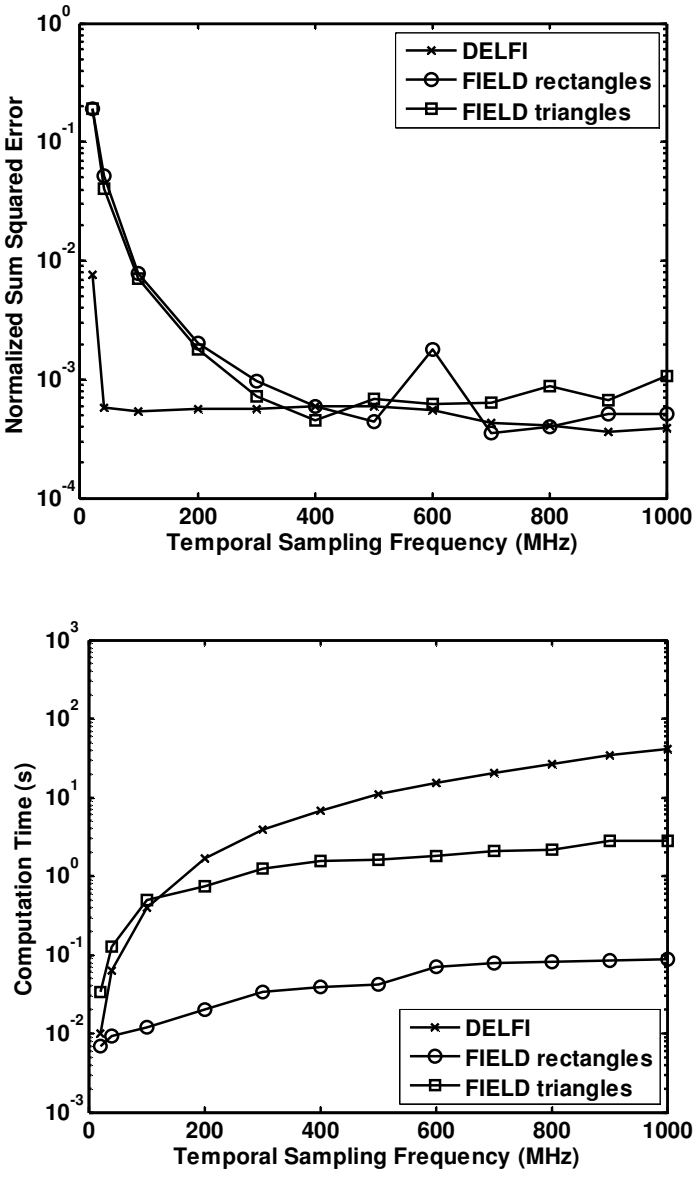

Figure 4:
Comparison of DELFI and FIELD II performance when computing space-time impulse responses over a range of temporal sampling frequencies. The top panel shows the normalized sum squared error with respect to FIELD II using triangles and sampled at 10GHz. The bottom panel shows the computation time for each of the codes. To achieve an error similar to that of DELFI sampled at 40 MHz, FIELD II using rectangles must be sampled at 400 MHz and FIELD II using triangles must be sampled at 300 MHz. Comparing computation times at these respective sampling rates, DELFI is about 1.7 times slower than FIELD II using rectangles and 19.4 times faster than FIELD II using triangles.

References:

[1] J. A. Jensen and N. B. Svendsen, "Calculation of pressure fields from arbitrarily shaped, apodized, and excited ultrasound transducers," *Ultrasonics, Ferroelectrics and Frequency Control, IEEE Transactions on*, vol. 39, pp. 262-267, 1992.

[2] J. W. Goodman, *Introduction to Fourier Optics*. San Francisco: McGraw-Hill, 1986.

[3] G. L. Wojcik, D. K. Vaughan, N. Abboud, and J. Mould, "Electromechanical modeling using explicit time-domain finite elements," presented at Proc. 1993 Ultrasonics Symposium, Baltimore, 1993.

[4] R. Barkman, W. Timm, S. Sakata, M. Heller, and C. C. Gluer, "Simulation of ultrasound interaction with bone structure based on 3D high-resolution-magnetic-resonance- and micro-CT-images," presented at Engineering in Medicine and Biology Society, 2000. Proceedings of the 22nd Annual International Conference of the IEEE, 2000.

[5] P. R. Stepanishen, "Transient Radiation from Pistons in an Infinite Baffle," *Journal of the Acoustical Society of America*, vol. 49, pp. 1629-1638, 1970.

[6] R. J. Zemp, C. K. Abbey, and M. F. Insana, "Linear system models for ultrasonic imaging: application to signal statistics," *IEEE Transactions on Ultrasonics Ferroelectrics & Frequency Control*, vol. 50, pp. 642-54, 2003.

[7] W. F. Walker, "The Significance of Correlation in Ultrasound Signal Processing," presented at SPIE International Symposium on Medical Imaging, San Diego, CA, 2001.

[8] D. A. Guenther, K. Ranganathan, M. J. McAllister, W. F. Walker, and K. W. Rigby, "Ultrasonic synthetic aperture angular scatter imaging," 2004.

[9] A. R. Selfridge, G. S. Kino, and B. T. Khuri-Yahub, "A theory for the radiation pattern of a narrow strip acoustic transducer," *Applied Physics Letters*, vol. 37, pp. 35-6, 1980.

[10] C. de Boor, *A Practical Guide to Splines*: Springer-Verlag, 1978.

[11] S. Haykin and B. Van Veen, *Signals and Systems*, 2 ed: Wiley, 2003.

[12] J. A. Jensen, "Ultrasound fields from triangular apertures," *The Journal of the Acoustical Society of America*, vol. 100, pp. 2049-2056, 1996.

[13] A. H. Nuttall, "Some Windows with Very Good Sidelobe Behavior," *IEEE Transactions on Acoustics, Speech, and Signal Processing*, vol. ASSP-29, pp. 84-91, 1981.

[14] F. Viola and W. F. Walker, "A spline-based algorithm for continuous time-delay estimation using sampled data," *Ultrasonics, Ferroelectrics and Frequency Control, IEEE Transactions on*, vol. 52, pp. 80-93, 2005.

[15] J. A. Hossack and G. Hayward, "Efficient calculation of the acoustic radiation from transiently excited uniform and apodised rectangular apertures," 1993.

[16] J. A. Jensen, "A New Calculation Procedure for Spatial Impulse Responses in Ultrasound," *Journal of the Acoustical Society of America*, vol. 105, pp. 3266-74, 1999.

Appendix:

The following equations are the analytical expressions resulting from the convolution of the two way impulse responses (7)-(12) with the cubic spline polynomial (13). For the sake of brevity, the cubic spline polynomial is convolved with only one of the summands in (7)-(12). The final analytical expressions for the impulse responses can be obtained through superposition with the results from the other summands.

$$
\begin{aligned}
&emm_{tr}(t) \underset{t}{*} h_{0_a} \underset{t}{*} h_{0_b} = \\
&\quad A_{0_a} A_{0_b} \sum_{j=M_0}^{M_1} \Big(\alpha_j + \beta_j \left(t - t_{0_a} - t_{0_b}\right) + \gamma_j \left(t - t_{0_a} - t_{0_b}\right)^2 \\
&\qquad + \delta_j \left(t - t_{0_a} - t_{0_b}\right)^3 \Big) \Big(u\left(t - t_{0_a} - t_{0_b} - j\partial\right) \\
&\qquad - u\left(t - t_{0_a} - t_{0_b} - (j+1)\partial\right) \Big)
\end{aligned}
\tag{A1}
$$

$$
\begin{aligned}
&emm_{tr}(t) \underset{t}{*} h_0 \underset{t}{*} h_1 = \\
&\quad A_0 A_1 \sum_{j=M_0}^{M_1} \Bigg[\alpha_j (t - t_1) + \frac{1}{2}\beta_j (t - t_1)^2 + \frac{1}{3}\gamma_j (t - t_1)^3 + \frac{1}{4}\delta_j (t - t_1)^4 \\
&\qquad + j\partial (t - t_1) \left(\beta_j + \gamma_j (j\partial + t - t_1) \right. \\
&\qquad \left. + \delta_j \left((j\partial)^2 + j\partial (t - t_1) + (t - t_1)^2 \right) \right) \Bigg] u(t - t_1) \\
&\qquad - \Bigg[\alpha_j (t - t_2) + \frac{1}{2}\beta_j (t - t_2)^2 + \frac{1}{3}\gamma_j (t - t_2)^3 + \frac{1}{4}\delta_j (t - t_2)^4 \\
&\qquad + (j+1)\partial (t - t_2) \left(\beta_j + \gamma_j \left((j+1)\partial + t - t_2 \right) \right. \\
&\qquad \left. + \delta_j \left(\left((j+1)\partial \right)^2 + (j+1)\partial (t - t_2) + (t - t_2)^2 \right) \right) \Bigg] u(t - t_2)
\end{aligned}
\tag{A2}
$$

where $t_1 = j\partial + t_0 + t_{10}$

$t_2 = (j+1)\partial + t_0 + t_{10}$

$$
\begin{aligned}
&emm_{tr}(t) \underset{t}{*} h_0 \underset{t}{*} h_2 = \\
&\quad A_0 A_2 \sum_{j=M_0}^{M_1} \Bigg[\frac{1}{2}\alpha_j (t-t_1)^2 + \frac{1}{6}\beta_j (t-t_1)^3 + \frac{1}{12}\gamma_j (t-t_1)^4 + \frac{1}{20}\delta_j (t-t_1)^5 \\
&\qquad + j\partial (t-t_1)^2 \left(\frac{1}{2}\beta_j + \gamma_j \left(\frac{j\partial}{2} + \frac{t-t_1}{3} \right) \right. \\
&\qquad \left. + \delta_j \left(\frac{(j\partial)^2}{2} + \frac{j\partial (t-t_1)}{2} + \frac{(t-t_1)^2}{4} \right) \right) \Bigg] u(t-t_1) \\
&\qquad - \Bigg[\frac{1}{2}\alpha_j (t-t_2)^2 + \frac{1}{6}\beta_j (t-t_2)^3 + \frac{1}{12}\gamma_j (t-t_2)^4 + \frac{1}{20}\delta_j (t-t_2)^5 \\
&\qquad + (j+1)\partial (t-t_2)^2 \left(\frac{1}{2}\beta_j + \gamma_j \left(\frac{(j+1)\partial}{2} + \frac{t-t_2}{3} \right) \right. \\
&\qquad \left. + \delta_j \left(\frac{((j+1)\partial)^2}{2} + \frac{(j+1)\partial (t-t_2)}{2} + \frac{(t-t_2)^2}{4} \right) \right) \Bigg] u(t-t_2)
\end{aligned}
\tag{A3}
$$

where $t_1 = j\partial + t_0 + t_{10}$

$t_2 = (j+1)\partial + t_0 + t_{10}$

$$
\begin{aligned}
&emm_{tr}(t) \underset{t}{*} h_{1_a} \underset{t}{*} h_{1_b} = \\
&\quad A_{1_a} A_{1_b} \sum_{j=M_0}^{M_1} \Bigg[\frac{1}{2}\alpha_j (t-t_1)^2 + \frac{1}{6}\beta_j (t-t_1)^3 + \frac{1}{12}\gamma_j (t-t_1)^4 + \frac{1}{20}\delta_j (t-t_1)^5 \\
&\qquad + j\partial (t-t_1)^2 \left(\frac{1}{2}\beta_j + \gamma_j \left(\frac{j\partial}{2} + \frac{t-t_1}{3} \right) \right. \\
&\qquad \left. + \delta_j \left(\frac{(j\partial)^2}{2} + \frac{j\partial (t-t_1)}{2} + \frac{(t-t_1)^2}{4} \right) \right) \Bigg] u(t-t_1) \\
&\qquad - \Bigg[\frac{1}{2}\alpha_j (t-t_2)^2 + \frac{1}{6}\beta_j (t-t_2)^3 + \frac{1}{12}\gamma_j (t-t_2)^4 + \frac{1}{20}\delta_j (t-t_2)^5 \\
&\qquad + (j+1)\partial (t-t_2)^2 \left(\frac{1}{2}\beta_j + \gamma_j \left(\frac{(j+1)\partial}{2} + \frac{t-t_2}{3} \right) \right. \\
&\qquad \left. + \delta_j \left(\frac{((j+1)\partial)^2}{2} + \frac{(j+1)\partial (t-t_2)}{2} + \frac{(t-t_2)^2}{4} \right) \right) \Bigg] u(t-t_2)
\end{aligned}
\tag{A4}
$$

where $t_1 = j\partial + t_{1_a 0} + t_{1_b 0}$

$t_2 = (j+1)\partial + t_{1_a 0} + t_{1_b 0}$

$$
\begin{aligned}
&emm_{tr}(t) \underset{t}{*} h_1 \underset{t}{*} h_2 = \\
&\quad A_1 A_2 \sum_{j=M_0}^{M_1} \left[\frac{1}{3}\alpha_j (t-t_1)^3 + \frac{1}{12}\beta_j (t-t_1)^4 + \frac{1}{30}\gamma_j (t-t_1)^5 + \frac{1}{60}\delta_j (t-t_1)^6 \right. \\
&\qquad + j\partial (t-t_1)^3 \left(\frac{1}{3}\beta_j + \gamma_j \left(\frac{j\partial}{3} + \frac{t-t_1}{6} \right) \right. \\
&\qquad \left. \left. + \delta_j \left(\frac{(j\partial)^2}{3} + \frac{j\partial (t-t_1)}{4} + \frac{(t-t_1)^2}{10} \right) \right) \right] u(t-t_1) \\
&\qquad - \left[\frac{1}{3}\alpha_j (t-t_2)^3 + \frac{1}{12}\beta_j (t-t_2)^4 + \frac{1}{30}\gamma_j (t-t_2)^5 + \frac{1}{60}\delta_j (t-t_2)^6 \right. \\
&\qquad + (j+1)\partial (t-t_2)^3 \left(\frac{1}{3}\beta_j + \gamma_j \left(\frac{(j+1)\partial}{3} + \frac{t-t_2}{6} \right) \right. \\
&\qquad \left. \left. + \delta_j \left(\frac{((j+1)\partial)^2}{3} + \frac{(j+1)\partial (t-t_2)}{4} + \frac{(t-t_2)^2}{10} \right) \right) \right] u(t-t_2)
\end{aligned}
\tag{A5}
$$

where $t_1 = j\partial + t_{10} + t_{20}$

$t_2 = (j+1)\partial + t_{10} + t_{20}$

$$
\begin{aligned}
&emm_{tr}(t) \underset{t}{*} h_{2_a} \underset{t}{*} h_{2_b} = \\
&\quad A_{2_a 0} A_{2_b 0} \sum_{j=M_0}^{M_1} \left[\frac{1}{4}\alpha_j (t-t_1)^4 + \frac{1}{20}\beta_j (t-t_1)^5 + \frac{1}{60}\gamma_j (t-t_1)^6 + \frac{1}{140}\delta_j (t-t_1)^7 \right. \\
&\qquad + j\partial (t-t_1)^4 \left(\frac{1}{4}\beta_j + \gamma_j \left(\frac{j\partial}{4} + \frac{t-t_1}{10} \right) \right. \\
&\qquad \left. \left. + \delta_j \left(\frac{(j\partial)^2}{4} + \frac{3j\partial (t-t_1)}{20} + \frac{(t-t_1)^2}{20} \right) \right) \right] u(t-t_1) \\
&\qquad - \left[\frac{1}{4}\alpha_j (t-t_2)^4 + \frac{1}{20}\beta_j (t-t_2)^5 + \frac{1}{60}\gamma_j (t-t_2)^6 + \frac{1}{140}\delta_j (t-t_2)^7 \right. \\
&\qquad + (j+1)\partial (t-t_2)^4 \left(\frac{1}{4}\beta_j + \gamma_j \left(\frac{(j+1)\partial}{4} + \frac{t-t_2}{10} \right) \right. \\
&\qquad \left. \left. + \delta_j \left(\frac{((j+1)\partial)^2}{4} + \frac{3(j+1)\partial (t-t_2)}{20} + \frac{(t-t_2)^2}{20} \right) \right) \right] u(t-t_2)
\end{aligned}
\tag{A6}
$$

where $t_1 = j\partial + t_{2_a 0} + t_{2_b 0}$

$t_2 = (j+1)\partial + t_{2_a 0} + t_{2_b 0}$

The following equations are the analytical calculations used to determine the times for the corners of the impulse response. These times are computed as projections of the corners of the element onto the line passing through the center of the element and the field point. The resulting times must be sorted as they don't take into account which element corner is closest to the field point. The element is assumed to be a rectangle lying in the XY plane of a Cartesian coordinate system, with its center at the origin. Here, n_x is the x-coordinate of the distance from element center to field point (n_y and n_z are such distance for their respective coordinates); $w_{0,x}$ is the x-coordinate for the element center, $w_{1,x}$ is the x-coordinate for the first element corner, $w_{2,x}$ is the x-coordinate for the second element corner, etc.; and c_0 is the speed of sound in the medium.

$$
\begin{aligned}
t_1 &= t_0 + \frac{n_x\left(w_{1,x}-w_{0,x}\right)+n_y\left(w_{1,y}-w_{0,y}\right)+n_z\left(w_{1,z}-w_{0,z}\right)}{\sqrt{n_x^{\,2}+n_y^{\,2}+n_z^{\,2}}*c_0} \\
t_2 &= t_0 + \frac{n_x\left(w_{2,x}-w_{0,x}\right)+n_y\left(w_{2,y}-w_{0,y}\right)+n_z\left(w_{2,z}-w_{0,z}\right)}{\sqrt{n_x^{\,2}+n_y^{\,2}+n_z^{\,2}}*c_0} \\
t_3 &= t_0 + \frac{n_x\left(w_{3,x}-w_{0,x}\right)+n_y\left(w_{3,y}-w_{0,y}\right)+n_z\left(w_{3,z}-w_{0,z}\right)}{\sqrt{n_x^{\,2}+n_y^{\,2}+n_z^{\,2}}*c_0} \\
t_4 &= t_0 + \frac{n_x\left(w_{4,x}-w_{0,x}\right)+n_y\left(w_{4,y}-w_{0,y}\right)+n_z\left(w_{4,z}-w_{0,z}\right)}{\sqrt{n_x^{\,2}+n_y^{\,2}+n_z^{\,2}}*c_0}
\end{aligned}
\qquad \text{(A7)}
$$

$$
\text{where } t_0 = \frac{\sqrt{n_x^{\,2}+n_y^{\,2}+n_z^{\,2}}}{c_0}
$$